ISSN 0965-545X, Polymer Science, Series A, 2016, Vol. 58, No. 6, pp. 975–986. © Pleiades Publishing, Ltd., 2016.

MEDICAL POLYMERS

Preparation, Optimization by 2^3 Factorial Design, Characterization and In Vitro Release Kinetics of Lorazepam Loaded PLGA Nanoparticles[1,2]

S. Bohrey*, V. Chourasiya, and A. Pandey**

Department of Chemistry, Dr. Harisingh Gour University, Sagar (M.P.), 470003 India

*e-mail: *s.bohrey@gmail.com, **prof.archnapandey@gmail.com*

Received November 30, 2015;
Revised Manuscript Received June 6, 2016

Abstract—The aim of this work was to formulate the lorazepam loaded poly(lactic-*co*-glycolic) acid (PLGA) nanoparticles by optimization of different preparation variables using 2^3 factorial design. The effect of three independent factors, the amount of polymer, concentration of the stabilizer and volume of organic solvent was investigated on two dependent responses, i.e., particle size and % drug entrapment efficiency. By using PLGA as polymer, PVA as a stabilizer and dimethyl sulfoxide as organic solvent lorazepam loaded PLGA nanoparticles were successfully developed through modified nanoprecipitation method. FTIR and DSC studies were carried out to examine the interaction between the excipients used and to explore the nature of the drug, the formulation and the nature of drug in the formulations. These nanoparticles were characterized for particle size, shape, zeta potential, % drug entrapment efficiency, % process yield and in vitro drug release behavior. In vitro evaluation showed particles size between 161.0 ± 5.4 and 231.9 ± 4.9 nm, % drug entrapment efficiency of formulations was in the range of 60.43 ± 5.8 to 75.40 ± 1.5, % process yield at 68.34 ± 2.3 to 81.55 ± 1.3 was achieved and in vitro drug release for these formulations was in the range of 49.2 to 54.6%. Different kinetics models, such as zero order, first order, Higuchi model, Hixson-Crowell model and Korsmeyer-Peppas model were used to analyze the in vitro drug release data. Preferred formulation showed particle size of 161.0 ± 5.4 nm, PDI as 0.367 ± 0.014, −25.2 mV zeta potential, drug entrapment efficiency as 64.58 ± 3.6% and 72.48 ± 2.5% process yield. TEM results showed that these nanoparticles were spherical in shape, and follow the Korsmeyer-Peppas model with a release exponent value of $n = 0.658$.

DOI: 10.1134/S0965545X1606002X

INTRODUCTION

Polymeric nanoparticles have attracted considerable interest as new vehicles for drug delivery, with the potential to overcome issues such as poor drug solubility and cell permeability [1]. The most important properties of nanoparticles are that they have a hydrophobic inner core and a hydrophilic outer shell. Their inner core is an appropriate reservoir for hydrophobic drugs [2]. Over the past few decades, researchers have focused on developing biodegradable nanoparticles as effective drug delivery devices [3]. For this purpose various polymers have been used such as chitosan [4], polylactic acid (PLA) [5], polyglycolic acid (PGA) and their copolymers, poly(lactic-*co*-glycolic) acid (PLGA) [6] etc.

PLGA is the one of the most successfully used biodegradable polymers amongst all these polymers, because the lactide/glycolide polymers chains are cleaved by hydrolysis into natural metabolites such as lactic acids and glycolic acids [7]. These are eliminated from the body as carbon dioxide and water by the tricarboxylic acid cycle, so a minimal systemic toxicity is associated with the use of PLGA for drug delivery or biomaterial applications [8]. PLGA is approved by the US FDA and European Medicine Agency (EMA) in various drug delivery systems in humans [9]. The polymers are commercially available with different molecular weights and copolymer compositions. The degradation time can vary from several months to several years, depending on the molecular weight and copolymer ratio. Forms of PLGA are usually identified by the monomers ratio used [10].

Properties such as good biocompatibility and biodegradability, low cytotoxicity and easy preparation are the reasons for the extensive use of polymeric nanoparticles prepared by PLGA as carriers for drugs, proteins, gene and vaccine delivery [11, 12]. There are several methods to prepare PLGA nanoparticles, namely: emulsion-solvent evaporation technique [13], double emulsion solvent evaporation technique [14], nanoprecipitation method [15], etc.

[1]The article is published in the original.

[2]Supplementary material is available at http://link.springer.com/.

Table 1. Different parameters used for 2^3 factorial design

Independent variables	Levels		Dependent variables
	Low	High	
Polymer amount, mg	50	100	Particle size, nm
Surfactant concentration, % w/V	1	1.5	Drug entrapment efficiency, %
Volume of organic solvent, mL	3	5	

The formulation design was generated by using Design Expert Software (Version 9.0).

Different organic solvents are utilized to dissolve the polymer and drug [16]. The aggregation of PLGA nanoparticles during nanoprecipitation method is a famed problem. Often the different polymer stabilizers are used to prevent PLGA nanoparticles aggregation. These stabilizers are coated on the surface of nanoparticles and can affect particle size, zeta potential and the surface properties. Many stabilizers such as poly(vinyl alcohol) (PVA) [17], PVA + chitosan [18], poloxamer 188 [19], poloxamer 407 [20], tween 60 [21], tween 80 [22], and so forth are utilized often. The literature suggests PVA as a most popular stabilizer for production of PLGA nanoparticles because it produced nanoparticles with smooth surface having negative charge. But it is not easy to remove excess amounts of PVA from the surface of nanoparticles by simple washing.

Lorazepam is 7-chloro-5-(2-chlorophenyl)-1,3-dihydro-3-hydroxy-2H-1,4-benzodiazepine-2-one (Scheme 1), having a formula $C_{15}H_{10}Cl_2N_2O_2$ belongs to a class of drugs known as benzodiazepines [23]. Benzodiazepines are amongst the most frequently used classes of medicinal drugs in the area of medication. [24]. Benzodiazepines are considered the treatment of choice for acute management of cruel seizures. Benzodiazepines are active against a wide range of seizure types, have a rapid onset of action once delivered into the central nervous system, and are safe [25]. Lorazepam has anxiolytics, sedative, hypnotics and anticonvulsants as well as muscle relaxant properties [26]. It is a poor water soluble substance. It could be administered via different routes: orally, intravenously, intramuscularly, and intranasal [27]. Generally, oral administration of lorazepam is the route of choice in the daily practice of pharmacotherapy.

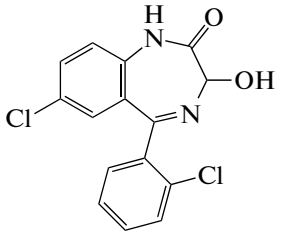

Scheme 1. Chemical structure of lorazepam.

Factorial design is a valuable technique to measure the combined effects of the independent variables. In the factorial design all the factors are studied in all the possible combinations, are believed to be the most efficient in estimating the influence of individual variables and their interactions using minimum experiments [28].

The purpose of this study was to develop, optimize and characterize lorazepam loaded polymeric nanoparticles based on biodegradable polymer for oral administration. Nanoparticles were synthesized by using modified nanoprecipitation method and the optimization of different variables was done by using 2^3 factorial design. The in vitro drug release was studied by dialysis bag method and the drug release data of drug loaded nanoparticles were examined by using various kinetic models such as zero order, first order, Higuchi model, Hixson-Crowell model and Korsmeyer-Peppas model.

EXPERIMENTAL

Materials

The biodegradable polymer studied was PLGA (RESOMER® RG 504 molecular weight range is (3.8–5.4) × 10^4 and inherent viscosity is 0.45–0.60 dL/g) with a copolymer ratio of dl-lactide to glycolide of 50 : 50 gifted from Evonik Mumbai (India). The surfactant used in this process was polyvinyl alcohol (PVA) purchased from Sigma-Aldrich, Mumbai (India). Lorazepam was received as a gift sample from Windlas Biotech Ltd, Dehradun (India). Purified water of Milli-Q quality was used to prepare the solutions as well as the aqueous phases of the emulsion. All other reagents and solvents were of analytical grade.

Experimental Design

Formulation design adopted in the study was the 2^3 factorial design. In this design two levels were decided such as for low values of variables as low level and for high values of variables as high level. Based on the results obtained in preliminary experiments, the independent variables of this design were as polymer amount in mg, surfactant concentration in % w/V of aqueous phase and volume of organic solvent. The dependent variables that were chosen for this experiment were particle size and drug entrapment efficiency. Details of this 2^3 factorial design are shown in Table 1.

Table 2. Experimental design and variables for 2^3 factorial design

Sample no.	Formulation batches	Amount of PLGA, mg	Concentration of PVA, % w/V of aqueous phase	Volume of organic solvent, mL
1	F_1	50	1	3
2	F_2	50	1	5
3	F_3	50	1.5	3
4	F_4	50	1.5	5
5	F_5	100	1	3
6	F_6	100	1	5
7	F_7	100	1.5	3
8	F_8	100	1.5	5

Preparation of Lorazepam Loaded PLGA Nanoparticles

The lorazepam loaded PLGA nanoparticles were prepared by using nanoprecipitation method [15], with minor modification (Scheme 2). Briefly, the organic phase was prepared by dissolving a typical amount of polymer and drug in dimethyl sulfoxide; sonicate it for 0.5 minutes by using an ultrasonic probe sonicator (Leela Electronics, Mumbai, India). The aqueous phase was prepared by dissolving a known amount of PVA in purified water of Milli-Q quality and sonicate it for 0.5 minutes. Then the organic phase was added into the aqueous phase by continuous sonication for a few minutes. The nanoparticles were immediately formed and organic solvent was then evaporated from the colloidal suspension by stirring at 300 RPM on magnetic stirrer (Remi, India) under atmospheric conditions for 4 hours. The suspension was centrifuged (WX ultra 100 ultracentrifuge Thermo Fisher Scientific USA) at 22000 RPM for 15 minutes to separate the nanoparticles from the free drug and excess surfactant. These nanoparticles were washed thrice with purified water of Milli-Q quality. The obtained nanoparticles suspension was used quickly for analysis or lyophilized (YSI-250, Yorco Freeze Dryer (Lyophilizer), Yorco Sales Pvt. Ltd., India). The formulation composition is summarized in Table 2.

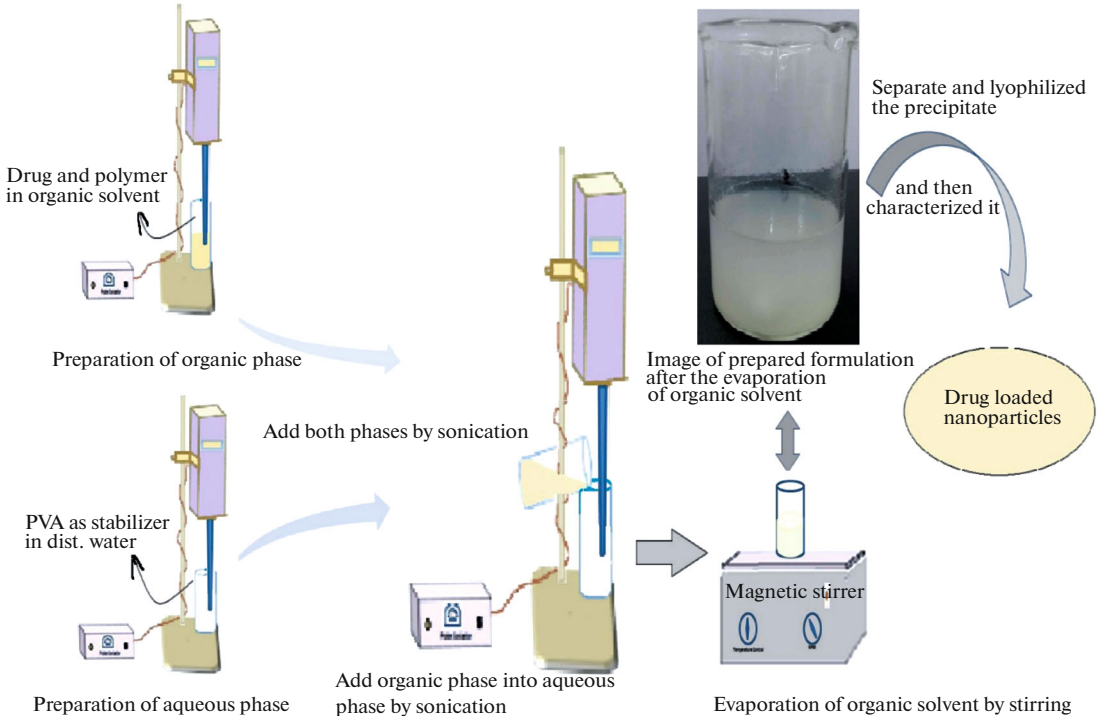

Scheme 2. Schematic representation of modified nanoprecipitation technique.

Fourier Transform Infrared Spectroscopy (FTIR)

FTIR was used to assess potential interactions between formulation components. The FTIR spectra of the polymer (PLGA), drug (Lorazepam) and lorazepam loaded PLGA nanoparticles were recorded on KBr pellets in the scanning range of 400–4000 cm^{-1}. These spectra were recorded on a FTIR-8400S Fourier Transform Spectrophotometer (Shimadzu, India).

Differential Scanning Calorimetry (DSC) Studies

DSC studies were also performed to assess the presence and nature of the encapsulated drug in formulations and also to study the interaction between excipients used. DSC studies were carried out in Jupiter NETZSCH STA 449F1A-0187-M. The samples were loaded in the chamber and gradually heated till 300°C with a heating rate of 10°C/min.

Particle Size Determination

Dynamic light scattering (DLS) analysis was performed for the determination of the particle size and size distribution of the drug loaded nanoparticles, for this purpose a Zetasizer (Model-ZEN 3600, Malvern Instruments, U. K.) was used. The dried powder samples were suspended in distilled water and slightly sonicated before analysis. The obtained homogeneous suspension was measured for the mean diameter and size distribution. Each measurement was performed in triplicate.

Zeta Potential

The zeta potential of a particle is the entire charge of the particle which is acquired by it in a particular medium. The zeta potential of nanoparticles was determined by using the Zetasizer (Model-ZEN 3600, Malvern Instruments, U.K.). In this technique, an electric potential was applied across a pair of electrodes at either end of a cell containing the particle dispersion. Charged particles were attracted to the oppositely charged electrode and their velocity was measured and expressed in unit field strength as their electrophoretic mobility. Samples in triplicate from the prepared suspensions were diluted in Milli-Q water and placed in the measurement cell for analysis.

Surface Morphology

Transmission electron microscopy (TEM) analysis, was done by using an instrument (TECNAI 200 KV TEM (Fei, Electron Optics) Japan) for the examination of the shape and size of drug loaded nanoparticles. For TEM analysis, a drop of the sample was placed on a Cu grid and the stained with 2% (wt/vol) phosphotungstic acid solution, and then the image was captured.

Atomic force microscopy (AFM) was also used to study the surface morphology. Atomic Force Microscope (INNOVA, ICON Analytical Equipment, Bruker, India) operating under the Acoustic AC mode (AAC or Tapping mode), with the aid of a cantilever (NSC 12(c) from MikroMasch, Silicon Nitride Tip) by NanoDrive™ version 8 software. The force constant was 2.0 N/m, while the resonant frequency was 284.60 kHz. The images were taken in air at room temperature, with the scan speed of 1.5–2.0 lines per seconds. The data analysis was done using Nanoscope Analysis software. The sample coated substrates was dried at the dust free space under 60 W lamp for 6 h followed by high vacuum drying and subsequently examined under AFM.

Drug Entrapment Efficiency and Process Yield

Nanoparticles were separated from dispersion by centrifugation at 22000 RPM for 15 minutes. The supernatant obtained after centrifugation was suitably diluted and analyzed for free lorazepam by UV–Vis spectrophotometer (Model no. 2201, UV–Vis double beam spectrophotometer, Shimadzu, India) at 327.2 nm. The percentage entrapment efficiency was calculated as:

$$\text{Entrapment efficiency, \%} = \frac{[\text{Drug}]_{\text{total}} - [\text{Drug}]_{\text{supernatant}}}{[\text{Drug}]_{\text{total}}} \times 100. \quad (1)$$

And the process yield of nanoparticles was calculated using the following equation:

$$\text{Process yield, \%} = \frac{\text{Weight of nanoparticle recovered}}{\text{Weight of (polymer + drug + surfactant)}} \times 100. \quad (2)$$

In Vitro Drug Release Study and In Vitro Drug Release Kinetics

In vitro drug release study of lorazepam loaded PLGA nanoparticles was analyzed by a dialysis bag diffusion method [29]. 2 mL of the sample was taken in dialysis bag and tied at both ends. It was immersed in a receptor compartment containing 100 mL of pH 7.4 phosphate buffer stirred at 100 RPM and temperature of 37 ± 1°C. The receptor compartment was covered with aluminium foil to prevent evaporation of the medium. 5 mL of the aliquots was withdrawn at various time intervals and replaced with fresh volume of phosphate buffer, diluted appropriately, and concentration of the drug was measured by UV–Vis double beam spectrophotometer (Shimadzu, 2201) at 327.2 nm. The experiments were performed in triplicate.

To analyze the in vitro drug release data various kinetic models were used to describe the release kinet-

Table 3. Particle size, % entrapment efficiency, % process yield and polydispersity index of prepared formulations F_1 to F_8

Sample no.	Code	Particle size, nm ± SD	% Entrapment efficiency ± SD	% Process yield ± SD	Polydispersity index ± SD
1	F_1	172.6 ± 6.2	60.43 ± 5.8	71.16 ± 3.7	0.302 ± 0.018
2	F_2	161.0 ± 5.4	64.58 ± 3.6	72.48 ± 2.5	0.367 ± 0.014
3	F_3	213.4 ± 5.3	63.02 ± 2.4	75.87 ± 3.1	0.297 ± 0.008
4	F_4	194.8 ± 8.5	68.27 ± 4.8	68.34 ± 2.3	0.565 ± 0.011
5	F_5	209.5 ± 4.1	69.63 ± 2.6	69.22 ± 1.8	0.264 ± 0.016
6	F_6	187.4 ± 5.8	72.45 ± 1.8	78.76 ± 2.4	0.450 ± 0.010
7	F_7	231.9 ± 4.9	70.27 ± 2.3	79.00 ± 1.8	0.348 ± 0.014
8	F_8	227.3 ± 6.7	75.40 ± 1.5	81.55 ± 1.3	0.492 ± 0.015

ics. The zero order rate Eq. (3) explains the systems where the rate of drug release does not depend on its concentration [30]. The first order Eq. (4) explains the release from the system where rate of drug release is concentration dependent [31]. Higuchi [32] described the release of drugs from insoluble matrix as a square root of time dependent process based on Fickian diffusion Eq. (5). Hixson-Crowell cube root law in Eq. (6) describes the release from systems where there is a change in surface area and diameter of particles [33]. Korsmeyer-Peppas et al. [34] derived a simple mathematical relationship which described the drug release from a polymeric system Eq. (7).

$$C = k_0 t, \tag{3}$$

where C is the concentration of drug at time t and k_0 is the zero-order rate constant expressed in units of concentration/time.

$$\log C_0 - \log C = k_1 t/2.303, \tag{4}$$

where C_0 is the initial concentration of drug and k_1 is the first order rate constant.

$$C = k_H \sqrt{t}, \tag{5}$$

where k_H is the constant reflecting the design variables of the system.

$$Q_0^{1/3} - Q_t^{1/3} = k_{HC} t, \tag{6}$$

where Q_t is the remaining amount of drug in the dosage form at time t, Q_0 is the initial amount of the drug and k_{HC} is the rate constant for Hixson-Crowell rate equation.

$$M_t/M_\infty = k_{KP} t^n, \tag{7}$$

where M_t/M_∞ is the fraction of drug released at time t, k_{KP} is the rate constant and n is the release exponent.

RESULTS AND DISCUSSION

The nanoprecipitation method with minor modification described here appeared to be a suitable technique to formulate lorazepam loaded PLGA nanoparticles with a size range below 200 nm in spherical shape with good entrapment efficiency and process yield. In typical nanoprecipitation method organic phase added to the aqueous phase by continuous stirring on a magnetic stirrer for better mixing of both phases and to give the nanoprecipitate. In the modified process, first we prepare the organic and aqueous phases by dissolving their components, respectively, then sonicate both phases separately for a few seconds. This step provides the perfect transparent solution, which reduces the size of the solution components. For the mixing of both phases we used ultrasonication, which provides high energy in a few minutes, so it reduces the process time. Another advantage of this modification is that the application of high energy results the maximum precipitation, so this increase the process yield in comparison of typical nanoprecipitation method.

All the factorial formulations were developed by the modified nanoprecipitation method using 2^3 factorial design. Different variables such as amount of polymer in mg, concentration of surfactant in the % wt/vol of the aqueous phase and volume of organic solvent in ml used in various formulations were summarized in Table 2. In each formulation composition of drug, aqueous phase volume and sonication time were fixed.

FTIR Analysis

FTIR analysis is a fundamental tool for the identification of chemical molecules and their interaction with each other [35]. The spectra for PLGA (in Fig. 1a) show peaks at 3358 cm^{-1} for O–H stretching, at 2950 cm^{-1} for C–H stretching, at 1765 cm^{-1} which is its characteristic peak due to the stretching of the carbonyl group, and at 1097 cm^{-1} for C–O stretching. The spectra for lorazepam drug (in Fig. 1b) show peaks at 3638 cm^{-1} for O–H stretching, at 3392 cm^{-1} for N–H stretching, at 3170 cm^{-1} for aromatic rings stretching, at 2960 cm^{-1} for C–H alkanes stretching, at 1655 cm^{-1} for C=O stretching, at 1083 cm^{-1} for C–N stretching and at for 796 cm^{-1} C–Cl stretching.

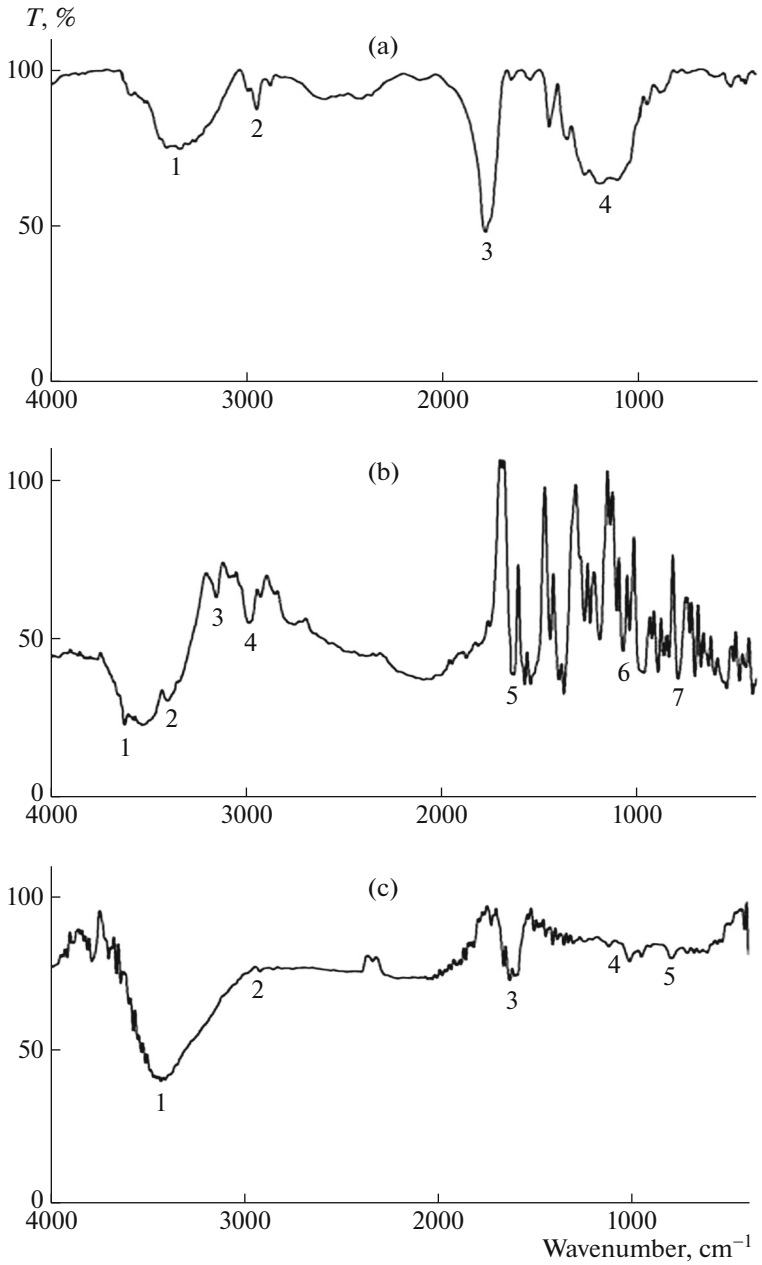

Fig. 1. FTIR spectra of (a) PLGA, (b) Lorazepam, and (c) Lorazepam loaded PLGA nanoparticles.

The FTIR spectra of lorazepam loaded nanoparticles (Fig. 1c), shows characteristic peaks of both polymer and drug such as at 3429 cm^{-1} for O–H stretching, 2933 cm^{-1} for C–H stretching, 1641 cm^{-1} for C=O stretching, 1099 cm^{-1} for C–N stretching and at for C–Cl 795 cm^{-1} stretching. This indicates no significant molecular interaction between lorazepam and PLGA.

DSC Studies

DSC thermograms of PLGA, lorazepam and lorazepam loaded nanoparticles are depicted in Fig. 2. The DSC thermogram of polymer showed a characteristic endothermic peak at 49.8°C (in Fig. 2a). The characteristic endothermic peak of lorazepam in DSC thermogram (in Fig. 2b) displayed at 186.9°C. DSC thermogram of lorazepam loaded nanoparticles showed two endothermic peak at 49.8 and 186.9°C attributed to polymer and drug (in Fig. 2c). The presence of both peaks in drug loaded nanoparticles indicating that lorazepam was encapsulated by the polymers in the nanoparticles.

Particle Size

The physicochemical, biopharmaceutical and drug release properties of the nanoparticles are affected by

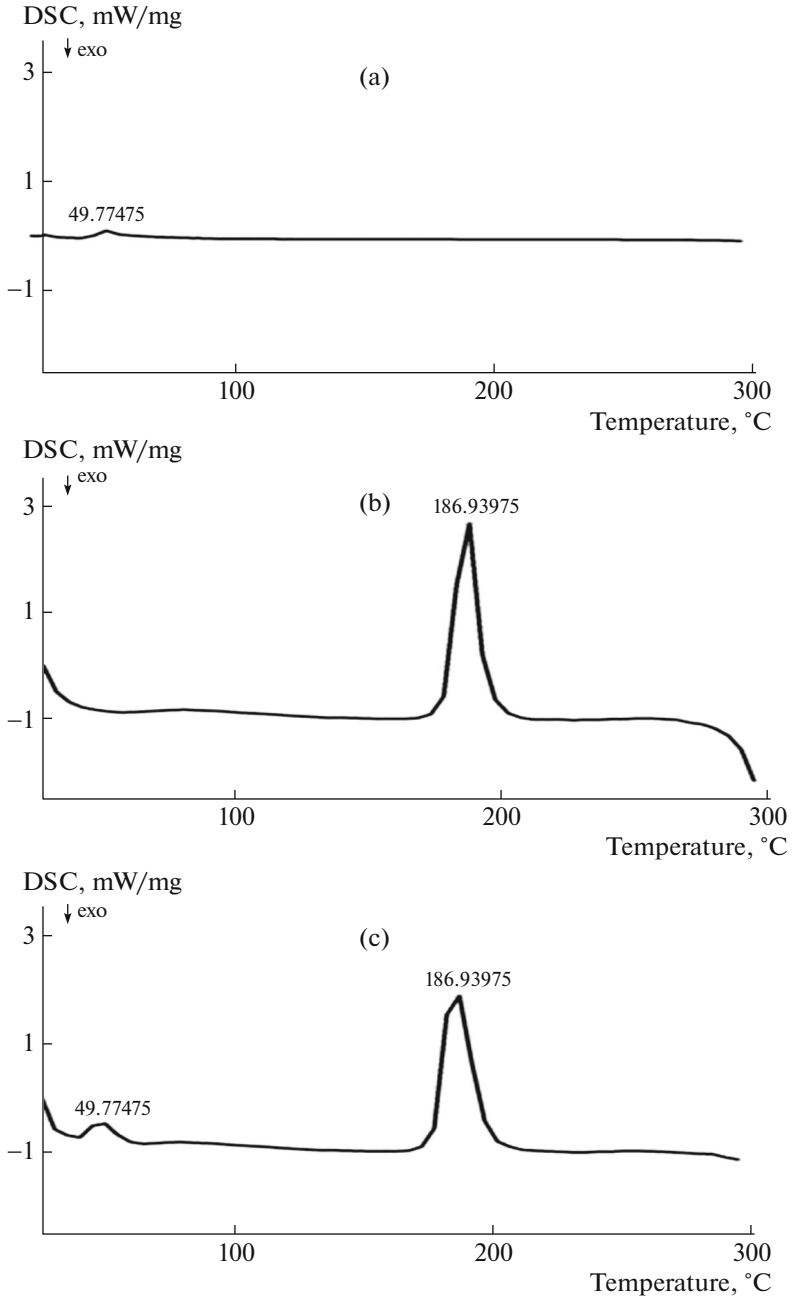

Fig. 2. DSC thermogram: (a) PLGA, (b) Lorazepam, and (c) Lorazepam loaded PLGA nanoparticles.

the size of particle [36]. The size of the particles is an epochal parameter because it has an apparent relevance to the formulation stability. Bigger particles have a tendency to aggregate to a greater extent in comparison to smaller particles, thereby resulting in sedimentation. The particle size of lorazepam loaded PLGA nanoparticles obtained is summarized in Table 3. The range of particle size was found from 161.0 ± 5.4 to 231.9 ± 4.9 nm.

The particles size of prepared nanoparticles was influenced by the concentration of PVA. According to the results, the nanoparticles with a smaller size range are obtained with low concentration of PVA. In the formulations with a low level of concentration of PVA F_1, F_2, F_5, and F_6, the particle size was found to be lower as compared to higher level PVA containing formulations F_3, F_4, F_7 and F_8. The cause for this was that, the function of the stabilizer is to stabilize the emulsion nanodroplets and protect them from coalescing with each other. For this reason a minimum amount of stabilizer is sufficient for efficient stabilization of nanodroplets [37]. The excess amount of sur-

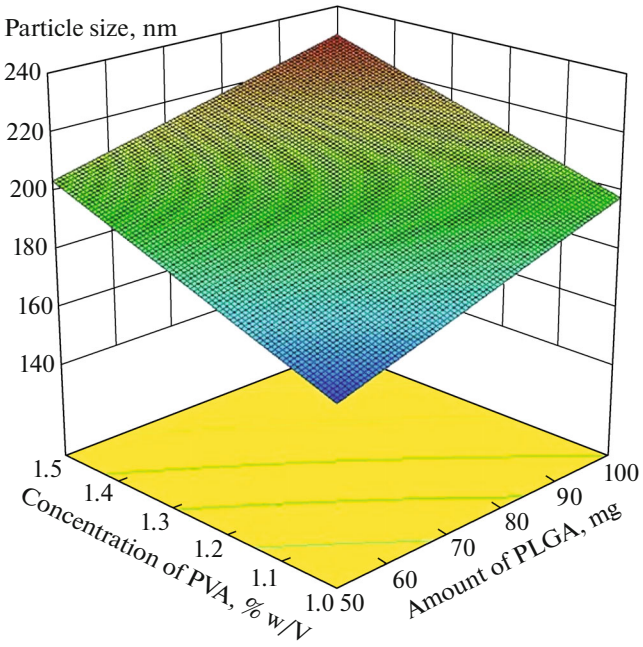

Fig. 3. (Color online) 3D surface plot depicting the effect of concentration of PVA and amount of PLGA on the particle size of nanoparticles.

factant increases the particle size because it is attached to the outer surfaces and the removal of excess stabilizer is a daunting task.

According to the result, the amount of PLGA was another significant factor which affects the particle size of nanoparticles. The particles size of formulations which prepared by the high level of polymer was to be higher than low level formulations. This was perhaps caused by the increasing viscous nature of dispersed phase, thus the diffusion of the organic phase into the aqueous phase is reduced; so it is responsible for the construction of bigger size particles. These results are similar as previous authors reported for the nanoprecipitation method [38].

The 3D surface plot shown in Fig. 3 explains the effect of PVA concentration and amount of PLGA on the particle size of nanoparticles. This shows that the stabilizer concentration and amount of polymer combination selected have better suitability to control the size of nanoparticles produced by using the modified nanoprecipitation technique. The DLS image of preferred formulation F_2 is shown in Fig. 4a.

Zeta Potential

Zeta potential of nanoparticles is a significant parameter which influences formulation stability. Samples were diluted appropriately using distilled water and sonicated for half minute before the measurement of zeta potential. Zeta potential value of preferred formulation F_2 was found to be −25.2 mV and graph is shown in Fig. 4b. High negative charge of zeta potential indicates that the electrostatic repulsion between particles with the same electric charge will prevent the aggregation of the particles [39].

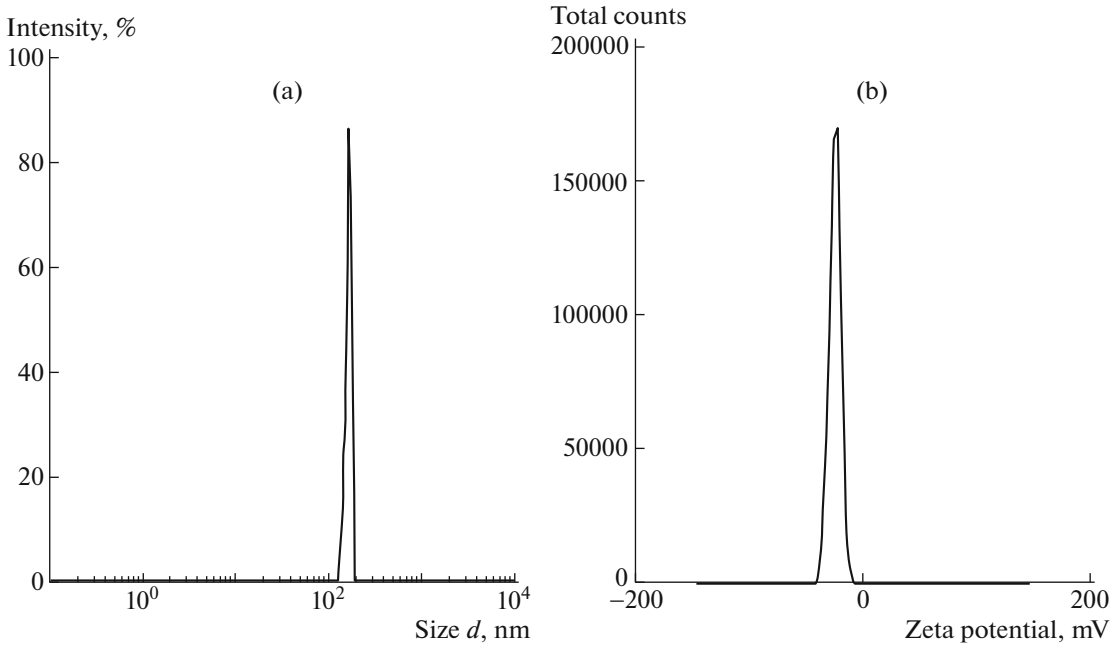

Fig. 4. (a) DLS image and (b) zeta potential graph of preferred formulation F_2.

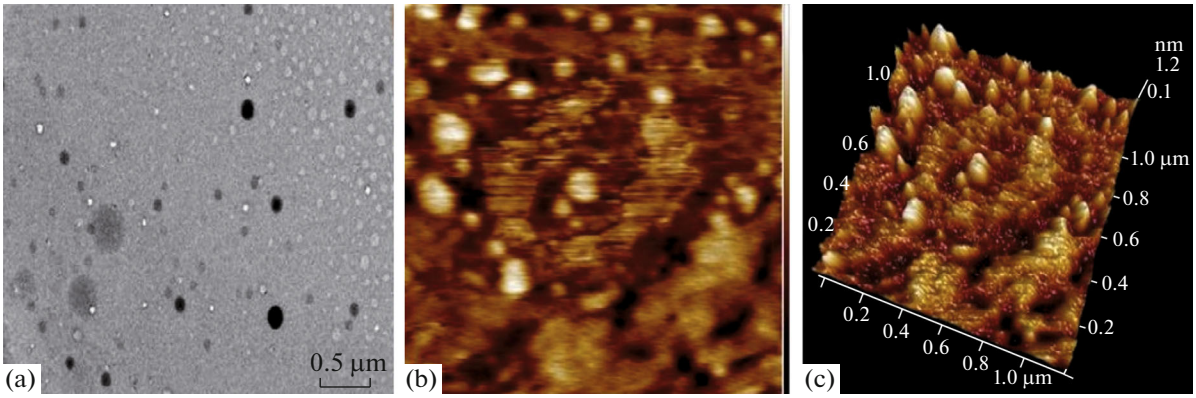

Fig. 5. (Color online) (a) TEM image, (b) AFM image, and (c) 3D view of AFM image of preferred formulation F_2.

Surface Morphology

Surface morphology of nanoparticles is another important parameter, which influences the drug release and drug absorbance properties. TEM and AFM analysis were performed for the evaluation of surface morphology of the prepared formulations. Examination of TEM images of the prepared nanoparticles revealed that these were spherical in shape and surfaces were smooth. TEM images of formulation F_2 were shown in Fig. 5a. The AFM image of preferred formulation F_2 was shown in Fig. 5b and its 3D view in Fig. 5c.

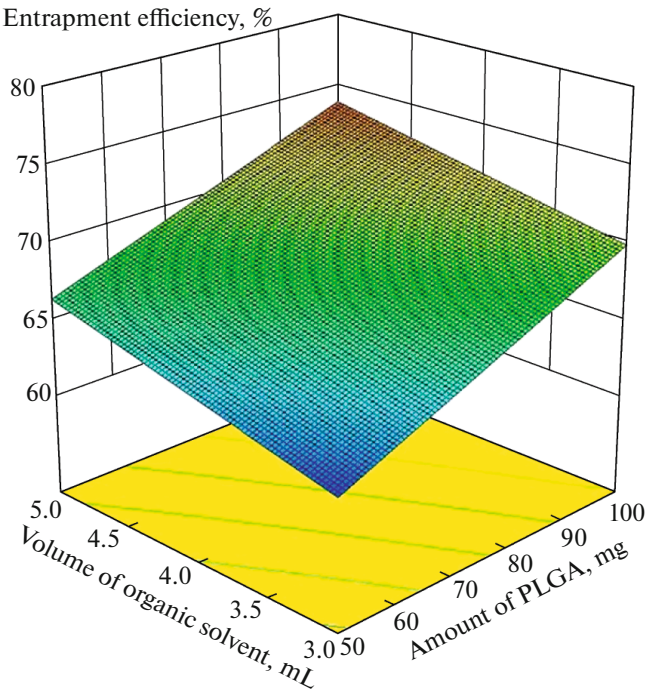

Fig. 6. (Color online) 3D surface plot illustrating the effect of amount of polymer and volume of organic solvent on the entrapment efficiency of nanoparticles.

Entrapment Efficiency and Process Yield

Entrapment efficiency of the formulation was in the range from 60.43 ± 5.8 to 75.40 ± 1.5%. Entrapment efficiency was found to be affected by the amount of polymer and the volume of organic solvent. The Entrapment efficiency of different formulation was shown in Table 3. Formulation F_8 containing 100 mg polymer, 1.5% w/V surfactant and 5 mL of organic solvent was found to possess high entrapment efficiency and formulation F_1 containing 50 mg polymer, 1% w/V surfactant and 3 mL of organic solvent was found to possess low entrapment efficiency.

Formulations F_5–F_8 were found to possess high entrapment efficiency and this may be due to the high level value of polymer and formulations F_1–F_4 containing low level value of polymer possesses low entrapment efficiency. According to these results, we can summarize that by increasing the amount of PLGA, entrapment efficiency also increases. This type of observation was also concluded by other authors [38].

The formulations containing low level value of organic solvent in composition show lower drug entrapment efficiency than the formulations containing high level value of organic solvent. This occurs due to the coalescence of droplets can be avoided by a large amount of organic solvent available for diffusion in the emulsion. The response surface plot depicting the effect of polymer and volume of organic solvent on the entrapment efficiency of nanoparticles shown in Fig. 6.

The examination of process yield is required to check the efficiency of the preparation method. If process yield is greater than 50%, then it is suitable for prepared formulations [40]. The process yield values for the prepared formulations are summarized in Table 3. This was found in range from 68.34 ± 2.3 to 81.55 ± 1.3%. The formulation F_8 shows good process yield 81.55 ± 1.3% and formulation F_4 shows low value

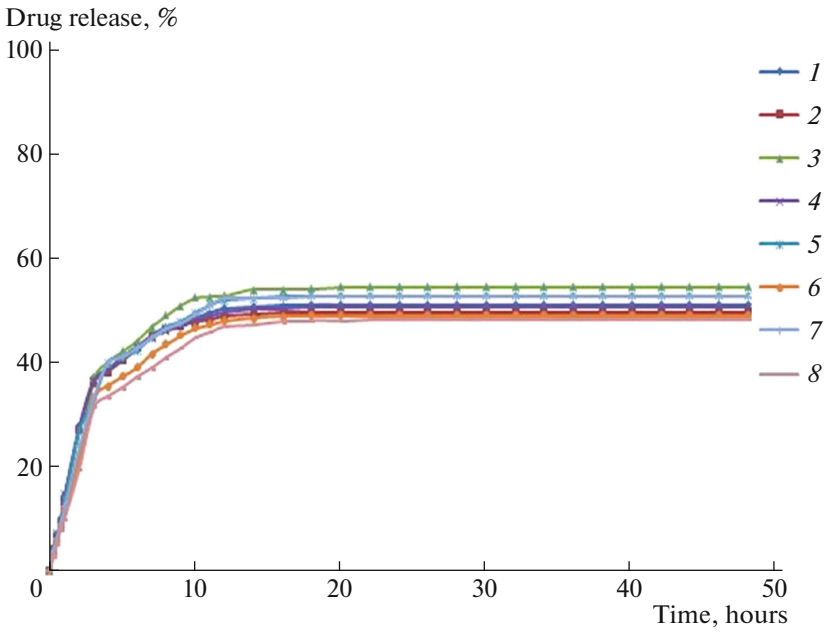

Fig. 7. (Color online) In vitro drug release of lorazepam from nanoparticles for different formulations: from (*1*) F_1 to (*8*) F_8.

of process yield as 68.34 ± 2.3%. This demonstrates the suitability of the method for prepared formulations.

In Vitro Drug Release Study and In Vitro Drug Release Kinetics

In vitro drug release studies were done by using the dialysis bag method. The drug release of different formulations is summarized in Fig. 7. This study showed biphasic release profile for all the formulations, initial burst release and followed by sustained release. Burst release was due to drug molecules adsorbed on the surface of nanoparticles. These drug particles at the surface instantaneously dissolve when it comes into with the medium [41].

For kinetic study following plots were made: cumulative % drug release vs. time (zero order kinetic model); log cumulative % drug remaining vs. time (first order kinetic model); cumulative % drug release vs. square root of time (Higuchi model); cube root of % drug remaining in matrix vs. time (Hixson–Crowell model); log cumulative % drug release vs. log time (Korsmeyer–Peppas model). All Plots are given in supplementary data and results are summarized in Table 4.

On the basis of best fit with the highest correlation (R^2) value it is concluded that the all formulation (F_1

Table 4. Release parameter for lorazepam loaded nanoparticles (F_1 to F_8) obtained by fitting in vitro drug release data to different models for drug release kinetics

F code	Zero order		First order		Higuchi model		Hixson–Crowell model		Korsmeyer–Peppas model		
	R^2	k	R^2	k	R^2	k	R^2	k	R^2	k	n
F_1	0.78310	7.9120×10^{-2}	0.81891	5.7213×10^{-3}	0.91298	1.6993	0.65519	2.7290×10^{-3}	0.97021	1.2175×10^{-2}	0.671
F_2	0.77216	6.9311×10^{-2}	0.80399	5.6257×10^{-3}	0.90532	1.5705	0.65254	2.7723×10^{-3}	0.97203	1.5237×10^{-2}	0.658
F_3	0.80113	7.6185×10^{-2}	0.83693	4.8793×10^{-3}	0.92304	1.7693	0.68291	2.7830×10^{-3}	0.97457	1.2857×10^{-2}	0.676
F_4	0.78210	7.8435×10^{-2}	0.81679	5.5490×10^{-3}	0.91251	1.7172	0.65449	2.7564×10^{-3}	0.97001	1.3147×10^{-2}	0.670
F_5	0.80553	8.0484×10^{-2}	0.84304	4.6518×10^{-3}	0.92748	1.9243	0.67471	2.7585×10^{-3}	0.97424	1.2869×10^{-2}	0.685
F_6	0.80743	7.8726×10^{-2}	0.83961	4.5282×10^{-3}	0.92779	1.7332	0.68257	2.7885×10^{-3}	0.97329	1.3128×10^{-2}	0.669
F_7	0.80504	8.0295×10^{-2}	0.84077	4.5996×10^{-3}	0.92651	1.9640	0.68	2.7503×10^{-3}	0.97504	1.2181×10^{-2}	0.674
F_8	0.82552	7.5337×10^{-2}	0.85817	4.1269×10^{-3}	0.93847	1.7649	0.69698	2.9167×10^{-3}	0.97342	1.2619×10^{-2}	0.679

to F_8) of nanoparticles follow the Korsemeyer–Peppas model, for preferred formulation F_2 correlation value $R^2 = 0.97203$ and release exponent value $n = 0.658$. The magnitude of the release exponent n indicates that the release mechanism is an anomalous transport or non Fickian diffusion, which is related to combination of both diffusion of the drug and dissolution of the polymer [31].

CONCLUSION

Lorazepam loaded PLGA nanoparticles were prepared successfully using the modified nanoprecipitation method. The results concluded that these formulations were found to be spherical in shape with narrow size distribution. In the described experimental conditions these formulations have good entrapment efficiency and process yield. The work demonstrated the use of 2^3 factorial design in optimizing preparation variables influencing the particle size and % entrapment efficiency of prepared formulations. We could achieve a maximum drug entrapment efficiency together with minimum particle size by performing less number of experiments. We could predict the particle size and % entrapment efficiency for various combinations of the preparation variables using the 3D surface plots. The in vitro drug release study shows sustained release of drug from the nanoparticles and follow the Korsmeyer–Peppas model and release mechanism is an anomalous transport or non Fickian diffusion, which is related to combination of both diffusion of the drug and dissolution of the polymer. Further in vivo studies are required to support the findings.

ACKNOWLEDGMENTS

The authors are very grateful to Windlas Biotech Ltd. Dehradun for providing a gift sample of lorazepam and Evonik Mumbai for providing the gift sample of PLGA. The facilities provided by Head, Department of Chemistry, and Head, Department of Pharmaceutical Science, Dr. Harisingh Gour University, Sagar (M.P.) are also acknowledged. The authors are also grateful to Electron Microscope Unit AIIMS, New Delhi for TEM analysis and Department of Pharmaceutical Science RGPV, Bhopal (M.P.) for analysis of DLS.

REFERENCES

1. Y. Yang, X. Y. Xie, and X. G. Mei, Drug Delivery **23** (3), 787 (2016).
2. D. H. Kim, M. D. Kim, C. W. Choi, C. W. Chung, S. H. Ha, C. H. Kim, Y. H. Shim, Y. I. Jeong, and D. H. Kang, Nanoscale Res. Lett. **7** (1), 91 (2012).
3. K. S. Soppimatha, T. M. Aminabhavia, A. R. Kulkarnia, and W. E. Rudzinski, J. Controlled Release **70**, 1 (2001).
4. J. You, W. Li, C. Yu, C. Zhao, L. Jin, Y. Zhou, X. Xu, S. Dong, X. Lu, and O. Wang, J. Nanopart. Res. **15**, 2123 (2013).
5. A. Kumari, S. K. Yadav, Y. B. Pakade, B. Singh, and S. C. Yadav, Colloids Surf., B **80**, 184 (2010).
6. P. Z. Milani, B. D. Loveymib, M. Jelvehgarid, and H. Valizadeh, Colloids Surf., B **103**, 174 (2013).
7. F. Danhier, E. Ansorena, J. M. Silva, R. Coco, A. L. Breton, and V. Preat, J. Controlled Release **161**, 505 (2012).
8. F. Y. Cheng, S. P. H. Wang, C. H. Su, T. L. Tsai, P. C. Wu, D. B. Shieh, J. H. Chen, P. C. H. Hsieh, and C. S. Yeh, Biomaterials **29**, 2104 (2008).
9. P. Verderio, P. Bonetti, M. Colombo, L. Pandolfi, and D. Prosperi, Biomacromolecules **14**, 672 (2013).
10. A. Prokop and J. M. Davidson, J. Pharm. Sci. **97**, 3518 (2008).
11. B. Wang, G. Chen, Z. Mao, Y. Zhang, D. Yu, and C. Gao, Chin. Sci. Bull. **57** (31), 3985 (2012).
12. M. Bao, Q. Zhou, W. Dong, X. Lou, and Y. Zhang, Biomacromolecules **14** (6), 1971 (2013).
13. Z. Hunter, D. P. McCarthy, W. Teck Yap, C. T. Harp, D. R. Getts, L. D. Shea, and S. D. Miller, ACS Nano **8** (3), 2148 (2014).
14. R. Surolia, M. Pachauri, and P. C. Ghosh, J. Biomed. Nanotechnol. **8**, 1 (2012).
15. H. Fessi, F. Puisieux, J. P. Devissaguet, N. Ammoury, and S. Benita, Int. J. Pharm. **55**, 1 (1989).
16. K. C. Song, H. S. Lee, I. Y. Choung, K. I. Cho, Y. Ahn, and E. J. Choi, Colloids Surf., A **276**, 162 (2006).
17. S. Bohrey, V. Chourasiya, and A. Pandey, Nano Convergence **3** (3), 1 (2016). doi 10.1186/s40580-016-0061-2
18. M. N. V. Ravi Kumar, U. Bakowsk, and C. M. Lehr, Biomaterials **25**, 1771 (2004).
19. B. Wang, X. C. Yu, S. F. Xu, and M. Xu, J. Nanobiotechnol. **13**, 22 (2015).
20. U. Bilati, E. All'emann, and E. Doelker, Eur. J. Pharm. Sci. **24**, 67 (2005).
21. H. Zhang, W. Cui, J. Bei, and S. Wang, Polym. Degrad. Stab. **91**, 1929 (2006).
22. D. T. Birnbaum, J. D. Kosmala, and L. B. Peppas, J. Nanopart. Res. **2**, 173 (2000).
23. B. Rezaei, M. K. Boroujeni, and A. A. Ensafi, Electrochim. Acta **123**, 332 (2014).
24. A. N. Zaid, R. J. Al-Ramahi, A. A. Ghoush, A. Qaddumi, and Y. A. Zaaror, Saudi Pharm. J. **21**, 71 (2013).
25. G. Abdelbary and R. H. Fahmy, AAPS PharmSciTech **10** (1), 211 (2009).
26. J. Ghasemi and A. Niazi, Anal. Chim. Acta **533**, 169 (2005).
27. S. Lissauer, J. Kenny, O. Jefferi, T. Wingfield, A. Miller, G. Chagaluka, L. Kalilani-Phiri, and E. Molyneux, Afr. J. Emerg. Med. **5**, 120 (2015).
28. B. Singh and N. Ahuja, Drug Dev. Ind. Pharm. **28**, 431 (2002).
29. Y. C. Kyo and J. F. Chung, Colloids Surf., B **83**, 299 (2011).
30. S. Dash, P. N. Murthy, L. Nath, and P. Chowdhury, Acta Pol. Pharm. **67** (3), 217 (2010).

31. P. Costa and J. M. Sousa Lobo, Eur. J. Pharm. Sci. **13**,123 (2001).

32. T. Higuchi, J. Pharm. Sci. **52**, 1145 (1963).

33. A. W. Hixson and J. H. Crowell, Ind. Eng. Chem. **23**, 923 (1931).

34. R. W. Korsmeyer, R. D. Gurny, E. M. Doelker, P. Buri, and N. A. Peppas, Int. J. Pharm. **15**, 25 (1983).

35. V. Chourasiya, S. Bohrey, and A. Pandey, Polym. Sci. Ser. B **57** (6), 645 (2015).

36. V. J. Mohanraj and Y. Chen, Trop. J. Pharm. Res. **5** (1), 561 (2006).

37. C. Vauthier and K. Bouchemal, Pharm. Res. **26**, 1025 (2009).

38. S. A. Joshi, S. S. Chavhan, and K. K. Sawant, Eur. J. Pharm. Bioharm. **76**, 189 (2010).

39. S. Feng and G. Huang, J. Controlled Release **71**, 53 (2001).

40. T. Govender, S. Stolnik, M. C. Garnett, L. Illum, and S. S. Davis, J. Controlled Release **57**, 171 (1999).

41. S. A. Agnihotri, N. N. Mallikarjuna, and T. M. Aminabhavi, J. Controlled Release **100**, 5 (2004).